Electrical percolation in quasi-two-dimensional metal nanowire networks for transparent conductors

Rose M. Mutiso and Karen I. Winey*
Department of Materials Science and Engineering, University of Pennsylvania, Philadelphia, Pennsylvania 19104, USA
(Received 27 June 2013; published 24 September 2013)

We simulate the conductivity of quasi-two-dimensional mono- and polydisperse rod networks having rods of various aspect ratios (L/D = 25–800) and rod densities up to 100 times the critical density and assuming contact-resistance dominated transport. We report the rod-size dependence of the percolation threshold and the density dependence of the conductivity exponent over the entire L/D range studied. Our findings clarify the range of applicability for the popular widthless-stick description for physical networks of rodlike objects with modest aspect ratios and confirm predictions for the high-density dependence of the conductivity exponent obtained from modest-density systems. We also propose a heuristic extension to the finite-width excluded area percolation model to account for arbitrary distributions in rod length and validate this solution with numerical results from our simulations. These results are relevant to nanowire films that are among the most promising candidates for high performance flexible transparent electrodes.

DOI: 10.1103/PhysRevE.88.032134 PACS number(s): 64.60.ah, 72.80.Tm

I. INTRODUCTION

Thin films of high-aspect-ratio conductive particles, such as carbon nanotubes, metal nanowires, and graphene flakes are of increasing interest for high performance solution processed flexible transparent conductors [1–3]. Random networks of metal nanowires are the highest performing materials among these emergent transparent conductor technologies, demonstrating optoelectronic properties on par with the ubiquitous indium tin oxide as well as compatibility with low-temperature solution processing and large-area deposition [2,3]. Computational and analytical studies of electrical percolation in two-dimensional (2D) random rod networks are of increasing interest in this field as they provide an important framework for understanding and predicting the dependence of electrical properties of nanotube and nanowire films on the nanoparticle sizes and network structure.

Percolation theory predicts that the electrical conductivity of a network of conducting particles scales with the particle loading by the power-law dependence shown below

$$\sigma \sim \left(\frac{N - N_c}{N_c}\right)^t, \tag{1}$$

where N is number density of the objects (or equivalently, their volume or area fraction), N_c is the critical number density of objects at the percolation threshold, and t is conductivity exponent. The power law in Eq. (1) is expected to hold at filler loadings above, but close to, the percolation threshold with a universal conductivity exponent $t_0 \approx 1.3$ in two dimensions [4]. To date, most theoretical studies of continuum percolation in two dimensions have focused on the random widthless-stick system [5–11] with particular emphasis on investigating the key critical phenomena, such as the percolation threshold and critical exponents as well as finite-size scaling behavior. The critical number of density of sticks at percolation N_c for the random widthless-stick system was obtained numerically via Monte Carlo simulations first by Pike and Seager [5] and recently by Li and Zhang [8] who reported a high precision value of the critical density $N_c L_{\text{stick}}^2 = 5.637\,26$, where L_{stick} is the stick length. Balberg *et al.* [12] and Balberg [13] related N_c to the particle geometry using excluded area arguments and numerical approximations to predict the dependency of the percolation threshold on the aspect ratio and orientation for both widthless and finite-width sticks. However, the complimentary simulations in their papers were limited to systems composed of small numbers of sticks ($<10^3$) and low-aspect ratios ($L/D < 15$) [6,13].

Recently, there has also been debate in the literature surrounding the nonuniversality of the conductivity exponent t in Eq. (1) observed first in experiments of nanotube-based films [14,15] and confirmed numerically by several studies [9,10,16] reporting a strong dependence of t on both stick density and the ratio of the contact and stick resistances (R_c/R_{stick}). On the other hand, the conductivity exponent extracted from the size dependence of the conductivity at the percolation threshold, as opposed to its density dependence in Eq. (1), yields the universal value of $t_0 \approx 1.3$ independent of the resistance ratio [9].

In this paper, we simulate the conductivity of quasi-2D random networks composed of soft-core rods that are confined to a plane. We perform the simulations over a very wide range of aspect ratios ($L/D = 25$–800) and rod densities up to $100N_c$ and assume contact-resistance dominated transport ($R_c \gg R_{\text{rod}}$). These simulated conductivities are then used to determine the percolation threshold and the density dependence of the conductivity exponent over the entire range of aspect ratios and rod densities studied. The objective of this paper is to evaluate: (1) the rod-size dependence of the percolation threshold as well as (2) the density dependence of the conductivity exponent. Previous numerical studies of these phenomena were based on the widthless-stick description [5,6,8] and modest-density systems ($N < 10N_c$) [7,9,10,16], respectively. The former objective is particularly relevant since the implicit assumption $L/D \to \infty$ for widthless sticks might not hold for many experimentally important modest-aspect-ratio systems. We also (3) study the effect of rod-size dispersity on the percolation threshold, proposing a heuristic extension to the finite-width excluded area percolation model to account for arbitrary

*winey@seas.upenn.edu

distributions in rod length and validating this solution with simulation results using the example of a network with a bi-disperse distribution of rod lengths. This paper builds upon our previous studies of percolation in isotropic and aligned networks of mono- and polydisperse three-dimensional (3D) networks [17–19] as well as a concurrent study [20] in which we integrated our simulation approach with experiments of well-defined metal nanowire films to produce quantitative predictions of the dependence of the sheet resistance on the nanowire size, areal density, and size dispersity.

II. SIMULATION METHOD

Our simulation method calculates the conductivity of quasi-2D rod networks as a function of the rod aspect ratio and nanowire density using a two-step approach. First, random assemblies of rods are generated using a Monte Carlo process, and a clustering analysis is performed to identify the percolated or spanning rod cluster. Second, the current across the sample is calculated using a random resistor network approach [21] to discretize the rod network, and Kirchoff's current law (KCL) equations are solved at each node. We have previously used this simulation approach in three-dimensional networks to explore the effects of rod orientation, aspect ratio, and size dispersity on the electrical conductivity and percolation threshold [17–19]. These simulations are relevant to polymer nanocomposites containing cylindrical nanofillers, such as carbon nanotubes and metal nanowires. In the current paper, we adapt our 3D simulation approach to model the sheet resistance of quasi-2D nanowire films by confining the rods to a thin film.

A random configuration of straight soft-core (i.e., interpenetrable) cylindrical rods is generated in a supercell of dimensions 1 unit by 1 unit by h. A confined quasi-2D structure is achieved by defining the height of the supercell $h = D_{\text{rod}}$, where D_{rod} is the diameter of the rods. The rods have isotropic orientation about the z axis but are confined in the x-y plane. Figure 1 shows a schematic of the configuration of the pseudo-2D simulation, whereas, representative renderings of the simulated rod networks are shown in the Supplemental Material [22]. Similar "single-layer" structures have been studied previously by Keblinski and Cleri [16] and Yi *et al.* [23] for soft-core fibers and ellipsoids, respectively. In this study, we simulate rod networks over a wide aspect-ratio range of L/D = 25–800. Three values of $h = D_{\text{rod}}$ are specified depending on the rod aspect ratio: D_{rod} = 0.000 25 u (unit) for L/D = 25–100, D_{rod} = 0.0001 u for L/D = 200–400, and D_{rod} = 0.000 05 u for L/D = 600–800. These values of D_{rod} are selected such that the normalized system size L_s, defined as the square length of the supercell (=1 u) normalized by the rod length

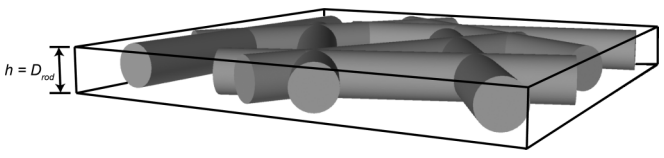

FIG. 1. Schematic of the quasi-2D simulation of rods (D_{rod},L_{rod}) contained in a volume of height h where $h = D_{\text{rod}}$. The soft-core rods have angular isotropy. Typical simulations contain ~3000–425 000 rods.

($L_s = L_{sq}/L_{\text{rod}}$), is $L_s \geqslant 25$ to minimize error from finite-size effects [9,10]. In this study, the normalized system size ranges between L_s = 25 and 160 depending on the L/D with L_s decreasing with increasing L/D. Simulations were performed for each aspect ratio at a range of rod densities defined by the volume fraction (ϕ). We compute the area fraction (A_f) of our quasi-2D networks based on the projected area of a rod (L_{rod}D$_{\text{rod}}$), specifically, $A_f = 4\phi/\pi$. Simulations involve ~3000–425 000 rods depending on the prescribed ϕ, L/D, and normalized system size L_s.

The supercell is divided into tiling sub-blocks, whose length is greater than the rod length, and rods that fall into each sub-block are registered. Aided by the sub-block data structures, the possible neighbors of each rod are determined with computational complexity that scales linearly with the total number of rods. Then, the shortest distance between the centers of two neighboring rods is calculated using a close-formed formula and, when this distance is $< D_{\text{rod}}$, the rods are in contact. A clustering analysis is then carried out to identify the percolating cluster of contacting rods that spans across the supercell, whereas, nonpercolating clusters are ignored. Every rod i in the percolating cluster is assigned a uniform voltage V_i (no internal resistance; $R_{\text{rod}} = 0$) that is an unknown variable, except for those rods that touch the left ($V_i = 1$) or right ($V_i = 0$) edges of the supercell. Assuming that all electrical resistance results from contact resistance R_c between contacting rods and writing KCL at each rod-rod junction, a system of linear equations is established. Here, one contact resistance R_c = 2 kΩ is assigned to all rod-rod junctions in the system. This assumption of uniform contacts has previously been applied to nanotube systems, even though the junction resistances are expected to vary widely due to the presence of both metallic and semiconducting carbon nanotubes [9,10,24–26] and is certainly more appropriate between metal nanowires. Note that the value of R_c = 2 kΩ is based on an estimate of the effective contact resistance between two silver nanowires obtained in our concurrent study by fitting simulated sheet-resistance values from our quasi-2D simulations to experimental data from well-defined silver nanowire films [20]. Furthermore, we assume contact-resistance dominated transport ($R_c \gg R_{\text{rod}}$) in our system. In our previous 3D simulations of rod networks in polymer nanocomposites [17–19], this assumption was reasonable since the polymer barrier between nanotubes or nanowires increases R_c significantly [17,27–29]. Similarly, high contact resistances are reported in metal nanowire networks associated with residual surfactant and/or poor conformation of contacting surfaces [30–32]. Postprocessing steps, such as thermal annealing, plasmonic welding, and electrochemical annealing can improve the quality of the contacts and can reduce R_c. Also, given that the length of metal nanowires used in transparent conductors is generally on the order of 5–20 μm, which is significantly larger than the mean free path of electrons ($\lambda \approx 30$ nm for Ag and $\lambda \approx 20$ nm for Cu [33]), R_{nw} can be significant. Naturally, the specifics of nanowire synthesis and nanowire film fabrication and processing can alter the applicability of our $R_c \gg R_{\text{rod}}$ assumption.

The system of linear equations established by applying KCL to all active junctions is then solved using the preconditioned conjugate gradient iterative method [34] as

implemented in the Portable, Extensible Toolkit for Scientific Computation package where the incomplete LU factorization preconditioner is used to obtain the cluster conductance. This entire procedure is repeated to obtain an ensemble-averaged conductance, achieving a standard deviation of less than 10% of the mean value in all cases. The conductivity of the rod network is calculated by normalizing the conductance by the dimensions of the supercell. For correspondence between simulation and physical units, we set $D_{\text{rod}} = 50$ nm in all cases, an experimentally typical value of the diameter of metal nanowires used for transparent conductors.

III. RESULTS AND DISCUSSION

A. Percolation thresholds from quasi-2D simulations

To extract the value of the critical area fraction at the percolation threshold (A_{fc}) for each rod aspect ratio studied, we apply Eq. (1) to our simulated conductivity values with A_{fc} and t as free variables, obtaining nonuniversal values of the conductivity exponent ($t \approx 1.4$–1.5) and high quality fits in all cases, Fig. 2(a). Note that A_{fc} and N_c notations are equivalent in Eq. (1), but we prefer the areal density notation for consistency with experiments. Power-law fits were applied over a narrow range of nanowire densities ranging between $A_f/A_{fc} \sim 1.1$ and 2, which is expected to fall within the critical region and, thus, to yield reliable estimates of the critical phenomena [9,13]. At loadings too close to the percolation threshold, finite-size errors are expected due to the divergence of the correlation length, whereas, loadings too far above the percolation threshold pull the system too far out of the critical region. Figure 2(b) shows the dependence of the critical area fraction as a function of the L/D of the rods, whereby each A_{fc} value was extracted from simulations as described above. As expected, we observe a dramatic reduction in the percolation threshold with increasing aspect ratio with an order of magnitude difference between the thresholds for $L/D = 25$ and 800. This finding is qualitatively consistent with numerical and theoretical results from widthless-stick systems where the critical number density of sticks (N_c) required to form percolated networks is inversely proportional to L^2_{stick} ($N_c \propto 1/L^2_{\text{stick}}$) [5,8,12]. Experimentalists have exploited the efficiency of high-(L/D) particles in network formation to produce nanowire films for highly conductive transparent electrodes at sufficiently low loadings required for high transparency [35–37], and new synthetic methods are being explored to produce ultrahigh-(L/D) nanowires to further improve properties [38,39].

To approximate the error in the thresholds presented in Fig. 2 associated with the finite size of our large simulations, finite-size scaling approaches were used to extrapolate the convergent threshold for an equivalent infinite system (A_{fc_inf}). The finite-size scaling behavior of the percolation threshold is described by

$$A_{fc} - A_{fc}(L_s) = L_s^{-(1/\nu)}\left[a_1 + a_2 L_s^{-\theta} + \cdots\right], \qquad (2)$$

where a_1 and a_2 are constants, $A_{fc}(L_s)$ is the system-size-dependent critical area fraction, $\nu = 4/3$ is the correlation length exponent in 2D, and θ is the first order correction-to-scaling exponent. Values of θ ranging between $\theta \approx 0.83$ and 0.9 have been reported for lattice percolation and continuum-stick systems [11,40–42]. In Fig. 3, we show $A_{fc}(L_s)$ as a function of the normalized system size for rods with $L/D = 800$ and $L_s = 5$–125. Fitting these data to Eq. (2), we find $A_{fc\_inf} = 0.007\,27$ and $\theta = 1.17$. This value of θ for our quasi-2D system is consistent with, but slightly larger than, the range of values reported in the literature for 2D square lattice and continuum systems. Furthermore, the value of $A_{fc\_inf} = 0.007\,27$ is only 1.23% smaller than the value of the threshold $A_{fc}(L_s = 25) = 0.007\,36$ extracted from the smallest system size used in Fig. 2(b). As finite-size errors in our system are expected to be most dominant for the highest L/D (= 800) and smallest system size ($L_s = 25$), we assume that the maximum error due to finite-size effects in our calculated thresholds over the entire L/D range studied will be on the order of ∼1%. This error is significantly smaller than the individual data points in Fig. 2(b). The low value of the maximum finite-size error in our simulated thresholds is also consistent with previous studies of

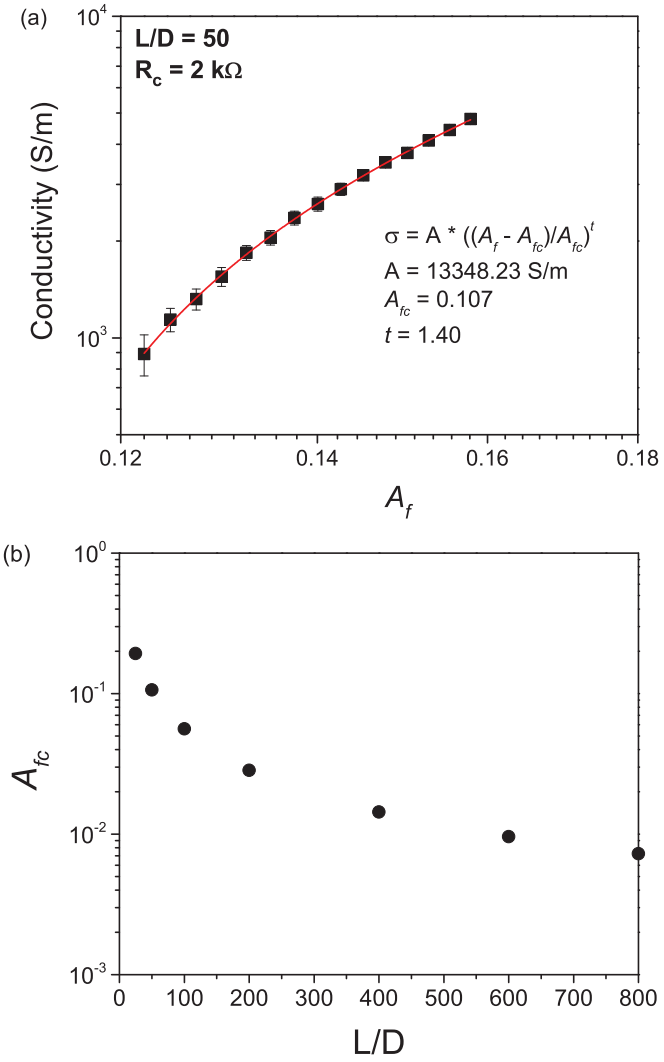

FIG. 2. (Color online) (a) Critical area fraction (A_{fc}) values are obtained by applying a power-law fit to simulated conductivity values over a narrow nanowire density range within the critical region ($1.1 < A_f/A_{fc} < 2$). A representative example for rods with $L/D = 50$ is shown. (b) Dependence of the critical area fraction (A_{fc}) extracted from simulations on the L/D of the rods.

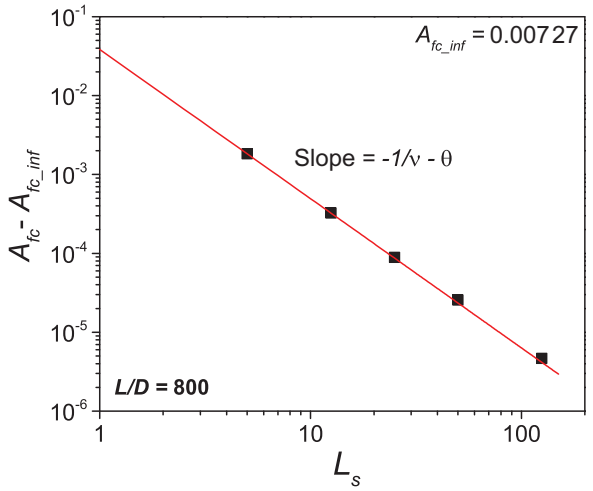

FIG. 3. (Color online) The system-size-dependent critical area fraction A_{fc}, obtained by power-law fits to simulated conductivity data, as a function of the normalized system size L_s for rods with $L/D = 800$. The data show power-law convergence to the percolation threshold for a corresponding infinite system A_{fc_inf}.

widthless-stick systems, which found that minimal finite-size effects are expected for very large square systems with $L_s > 20$ [8–11]. This result further corroborates the reliability of our simulated conductivities and calculated thresholds presented in Fig. 2. Also, Fig. 3 shows, to leading order, a power-law convergence of $A_{fc}(L_s)$ to A_{fc_inf} with an exponent of $-1/\nu - \theta$ as expected since the prefactor a_1 in Eq. (2) is significantly smaller than a_2 for a symmetric system in 2D (cf. Ref. [11]).

B. Comparison with models

Next, we compare our simulated thresholds to predictions from the excluded area model and the widthless-stick result. Rodlike objects in 2D can be modeled as finite-width or widthless sticks with the former case approaching the latter with increasing aspect ratio. The finite-width-stick description is most consistent with our quasi-2D simulations of confined networks composed of rods with projected area $L_{\text{rod}}D_{\text{rod}}$. Furthermore, the widthless-stick description is inappropriate for experimental nanowire films at modest nanowire aspect ratios as will be shown later in this section.

The excluded area and excluded volume are widely used concepts to describe the onset of percolation as a function of the filler geometry in two and three dimensions, respectively. In two dimensions, the excluded area A_{ex} is the area around an object into which the center of another identical object cannot enter without contacting the first object [12,43]. In a system of many objects, the average excluded area per object $\langle A_{ex}\rangle$ is defined by taking the average over all possible relative orientations. At percolation, the total excluded area is defined as

$$\langle A_{ex\_tot}\rangle = N_c \langle A_{ex}\rangle . \tag{3}$$

The total excluded area (or volume) is a dimensional invariant only for a system of all-parallel soft-core objects [12]. In three-dimensional rod networks, the total excluded volume ranges between the all-parallel value of 2.8 and the slender-rod-limit value of 1, exhibiting a strong dependence on the aspect ratio for the nonparallel systems [17,44,45]. In two dimensions, $\langle A_{ex\_tot}\rangle = 4.5$ for parallel objects, whereas, $\langle A_{ex\_tot}\rangle = 3.4 - 4.1$ has been reported for isotropic assemblies of soft-core ellipses, widthless sticks, and capped rectangles [12,13,46].

The average excluded area per object in a system of randomly oriented soft-core finite-width sticks with length L and width D is given by [12]

$$\langle A_{ex}\rangle = 2LD\left(1+\frac{4}{\pi^2}\right) + (L^2+D^2)\frac{2}{\pi}. \tag{4}$$

Following from Eqs. (3) and (4), the critical area fraction for a system of randomly oriented finite-width sticks is

$$A_{fc} = N_c A = \frac{\langle A_{ex\_tot}\rangle}{\left(2+\frac{8}{\pi^2}\right) + \left(\frac{L}{D}+\frac{D}{L}\right)\frac{2}{\pi}}, \tag{5}$$

where $A = LD$ is the area of the rectangular stick. We estimate $\langle A_{ex\_tot}\rangle$ using our simulated thresholds from Fig. 2(b) in Eq. (3), observing a weak dependence of this value on the aspect ratio of the rods over the entire L/D range with a mean value of $\langle A_{ex\_tot}\rangle \approx 3.7$ (Fig. 4). For comparison, reported [12] $\langle A_{ex\_tot}\rangle$ for the random widthless-stick system is 3.57. Moreover, Xia and Thorpe [46] observed a similar weak dependence of the total excluded area ($\langle A_{ex\_tot}\rangle \approx 3.5$) on the aspect ratio in their study of percolation in random systems of overlapping ellipses when the aspect ratio was varied between ~20 and 400. In Fig. 5(a), we compare our simulated thresholds [replotted from Fig. 2(b)] to predictions from the finite-width-stick excluded area model calculated using Eq. (5) with $\langle A_{ex\_tot}\rangle = 3.7$ and observe excellent agreement between the two. In contrast, the widthless-stick result $\left(N_c L^2_{\text{stick}} = 5.637\,26\right)$ agrees with both our simulation results and the finite-width model only when $L/D > 100$, see Fig. 5(b), demonstrating that the widthless-stick description is inappropriate for networks with modest-aspect-ratio fillers.

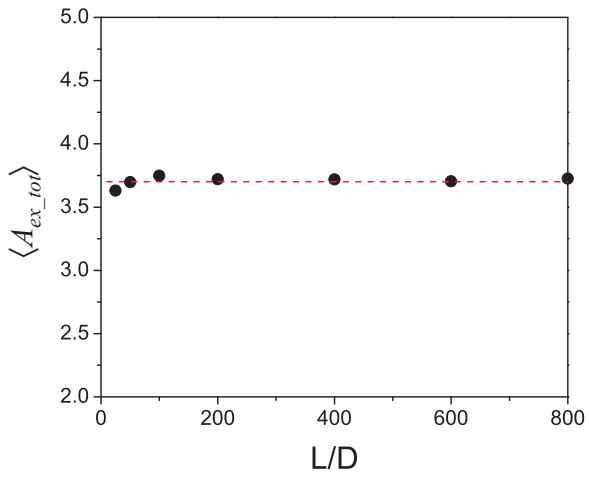

FIG. 4. (Color online) The total excluded area $\langle A_{ex\_tot}\rangle$ calculated from our simulated thresholds using Eq. (2) (points) as a function of L/D shows weak dependence on the rod aspect ratio. The dashed line shows the mean value of $\langle A_{ex\_tot}\rangle = 3.7$.

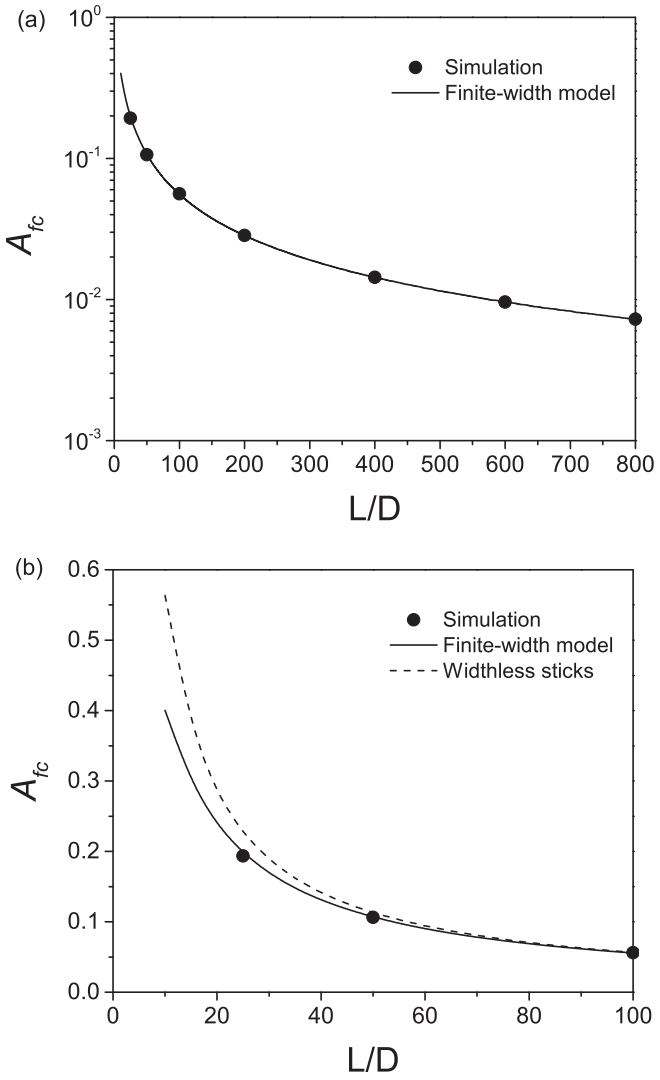

FIG. 5. (a) Simulation (points) and finite-width excluded area model predictions [Eq. (5)] (solid line) for A_{fc} of isotropic quasi-2D rod networks as a function of L/D. (b) Comparison of results from simulation and the finite-width excluded area model with predictions from the widthless-stick system (dashed line) at $L/D \leqslant 100$. The 2D widthless-stick approximation when applied to nanowire films is most reliable for nanowires with sufficiently high L/D's.

C. The conductivity exponent

In this paper, we study the conductivity exponent t from Eq. (1) as a function of the rod aspect ratio and density in a contact-resistance dominated system ($R_c \gg R_{\text{rod}}$) over a very large range of aspect ratios (L/D = 25–800) and nanowire densities ($0.1 < N < 100N_c$). Balberg *et al.* [7] determined, for the first time, the conductivity exponent for a 2D system of randomly distributed conducting sticks, finding a value of $t = 1.24 \pm 0.03$, in reasonable agreement with the universal value of $t_0 \approx 1.3$. In quasi-2D networks of fibers confined to a plane, Keblinski and Cleri [16] showed that the universal power law holds only for low-stick densities $N < 2N_c$, whereas, at higher concentrations (up to $10N_c$), t transitions to a value of either 1 or 1.75 for stick- and contact-resistance dominated transport, respectively. Similarly, Li and Zhang [9] simulated the dependence t on R_c/R_{stick} in a random widthless-stick system over a narrow range of $N < 2N_c$, observing a monotonic increase in t with increasing R_c/R_{stick}. A maximum value of $t \approx 1.42$ was reported for $R_c/R_{\text{stick}} \geqslant 10^2$, and a minimum value of $t \approx 1.2$ was reported for $R_c/R_{\text{stick}} \leqslant 10^{-2}$. These results are consistent with Žeželj and Stanković [10] who observe that the conductivity exponent converges to the universal value at the percolation threshold irrespective of R_c/R_{stick} in random networks of widthless sticks and takes on a range of values $1 \leqslant t \leqslant 2$ depending on the stick density and R_c/R_{stick}. Here, when $N \gg N_c$, t converges towards a value of 2 in the limit of superconductive sticks ($R_c \gg R_{\text{stick}}$) and 1 in the limit of superconductive junctions ($R_{\text{stick}} \gg R_c$). Žeželj and Stanković [10] credit this (R_c/R_{stick})-dependent behavior of t to the structure of dense networks, wherein most of the sticks in the system contribute to the conductivity. Thus, the density of the current-carrying sticks is directly proportional to the stick density, and the density of current-carrying contacts is proportional to the square of the stick density, the latter case arising from the proportionality between the number of contacts per stick and the total number of sticks in the system. In contrast to the current paper, which simulates rod densities up to $100N_c$ and a wide range of L/D = 25–800, these previous studies of the electrical conductivity exponent in 2D were limited to modest-density systems ($N < 10N_c$), and the sole study addressing finite-width rods [16] was limited to $L/D \approx 50$. For completeness, also note that a rigorous finite-size scaling analysis similar to Eq. (2) is required to extrapolate the critical conductivity exponent t_0 at $N = N_c$. An example of this procedure is provided in the Supplemental Material [22] for rod networks with $L/D = 800$, yielding $t_0 = 1.36$, close to the expected universal value of $t_0 \approx 1.3$. The discussion in the remainder of this section is limited to the exponent t from Eq. (1), which is of particular interest in the study of the electrical properties of various nanowire- and nanotube-based experimental systems.

Figure 6 shows a log-log plot of the simulated conductivity versus the reduced rod number density $[(N - N_c)/N_c]$ for

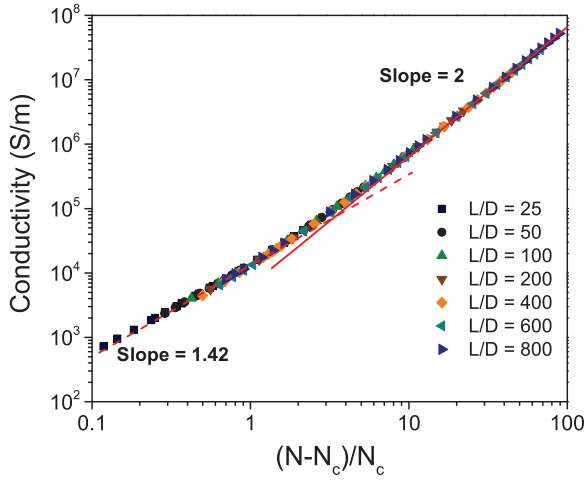

FIG. 6. (Color online) Simulated conductivity versus the reduced rod number density $[(N - N_c)/N_c]$ for L/D = 25–800 and rod density up to $100N_c$ in a contact-resistance limited system ($R_c \gg R_{\text{rod}}$). For all L/D studied, $t = 1.42$ at low densities ($N/N_c < 2$), and $t = 2$ at high densities ($N/N_c > 10$). Error bars are smaller than the points.

L/D = 25–800 where the value of the percolation threshold for each aspect ratio is given in Fig. 2(b) and is converted to number density notation. The slope gives the conductivity exponent t. Across the entire L/D range, the data show power-law behavior with an exponent of $t = 1.42$ at low densities ($N/N_c < 2$) and $t = 2$ at high densities ($N/N_c > 10$) with a crossover region at intermediate densities $2 < N/N_c < 10$. The low-density behavior is consistent with the finding of Li and Zhang [9] that $t \approx 1.42$ for a contact-resistance dominated network with $N < 2N_c$ as well as with Žeželj and Stanković [10] who report a value of the local density-dependent conductivity exponent of $t(N) \sim 1.4$–1.5 at $N \sim 2N_c$ when $R_c > R_{\text{stick.}}$ In addition, the high-density behavior in Fig. 5 is consistent with predicted convergence to $t = 2$ for $R_c \gg R_{\text{rod}}$ and $N \gg N_c$reported by Žeželj and Stanković [10] and Keblinski and Cleri [16], although neither of these studies investigated sufficiently high rod densities to observe a value of $t = 2$.

The results presented in Fig. 6 are significant by verifying the high-density ($N \gg N_c$) behavior of the conductivity exponent as predicted from modest-density systems [10,16] and showing the invariance of t with rod size in quasi-2D rod networks.

D. Size dispersity

We previously demonstrated the capability of our simulation method to simulate the conductivity of random three-dimensional soft-core rod networks with arbitrary distributions in rod size [17]. We also determined a percolation threshold from our simulations of polydisperse rods with experimentally typical Gaussian distributions in length and diameter as well as engineered bi-disperse mixtures of low- and high-aspect-ratio rods [17]. Furthermore, using empirical approximations from our simulation data, we generalized the widely used slender-rod-limit excluded volume percolation model to account for both finite L/D and arbitrary size dispersity. Here, we extend this approach to study the effect of rod-size dispersity on the percolation threshold in 2D using the example of a rod network with a bi-disperse distribution of rod lengths. These networks exploit the dominant contribution of high-(L/D) fillers in network formation (Figs. 2 and 5), whereas, capitalizing on the availability and processability of modest-(L/D) particles. This is particularly relevant in nanowire films for transparent conductor applications whereby very high L/D (>400) is required to meet performance criteria for many critical applications [20]. To simulate a bi-disperse network, we define reference rods with $L/D = 50$ ($L_{\text{Ref}} = 0.0125$ u and $D_{\text{Ref}} = 0.000\,25$ u) and longer high-(L/D) rods with $L/D = 400$ ($L_{\text{Long}} = 0.1$ u and $D_{\text{Long}} = D_{\text{Ref}}$) where the rod-length ratio is $r_L = L_{\text{Long}}/L_{\text{Ref}} = 8$. The proportion of longer rods in the network is expressed as a relative area fraction $F_{\text{Long}} = A_{f\_Long}/(A_{f\_Ref} + A_{f\_Long})$ and is varied between $F_{\text{Long}} = 0$ (monodisperse; $L/D = 50$) and $F_{\text{Long}} = 1$ (monodisperse; $L/D = 400$). Similar to the monodisperse case, $R_c = 2$ kΩ for all rod junctions in the network and $R_{\text{rod}} = 0$, and percolation thresholds are extracted from the simulated conductivities by applying the power-law fit in Eq. (1). We plot the percolation threshold of our simulated bi-disperse rod networks as a function of F_{Long} = 0, 0.2, 0.5, 0.8, and 1 (Fig. 7). As expected, we observe a significant reduction in A_{fc} with an increasing fraction of high-(L/D) rods in the network.

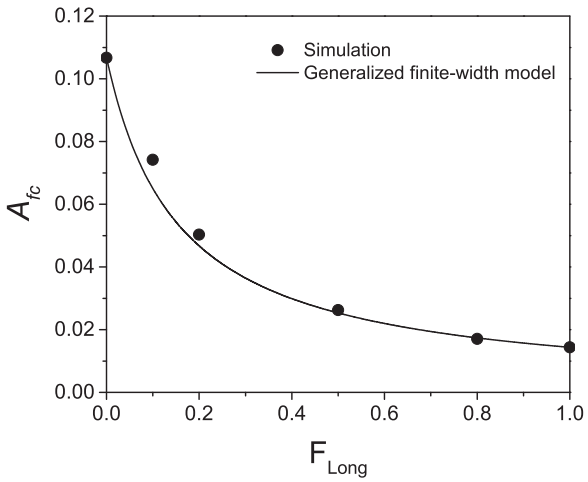

FIG. 7. A_{fc} as a function the relative area fraction of long rods (F_{Long}) in bi-disperse quasi-2D rod networks containing a mixture of short rods with $L/D = 50$ and long rods with $L/D = 400$. Simulated results (points) agree well with predictions from our generalized finite-width excluded area model [Eq. (5)] (line).

Next, we propose a heuristic generalization of the excluded area model solution for monodisperse rods [Eq. (5)] to predict the percolation threshold for isotropic networks of rods with arbitrary distributions in length by taking the average of Eq. (5),

$$A_{fc\_poly} = \frac{\langle A_{ex\_tot}\rangle \langle L\rangle_n D}{2\langle L\rangle_n D\left(1+\frac{4}{\pi^2}\right)+(\langle L^2\rangle_n + D^2)\frac{2}{\pi}} = \frac{\langle A_{ex\_tot}\rangle}{\left(2+\frac{8}{\pi^2}\right)+\left(\frac{\langle L\rangle_w}{D}+\frac{D}{\langle L\rangle_n}\right)\frac{2}{\pi}}, \quad (6)$$

where the subscripts n and w denote weight and number averages, respectively, and $\langle A_{ex\_tot}\rangle = 3.7$. Note that, for quasi-2D single-layer confined networks, D defines the system height, and thus, dispersity in D is not allowed. The $D/\langle L\rangle_n$ term in the denominator of Eq. (6) is negligibly small at low L/D and vanishes as L/D increases, thus, the expression is dominated by the weight average term L_w. Others have observed a weight average dependence of the percolation threshold on the rod length in three dimensions [17,47–50], and this result is intuitive since higher L/D rods in the polydisperse network play a more critical role in network expansion. Figure 7 shows there is excellent agreement between our simulations and predictions from our generalized finite-width excluded area model expression [Eq. (6)]. Our generalized expression in Eq. (6) provides a convenient and accessible solution for the percolation threshold of confined random networks of rods with arbitrary distributions in length.

IV. CONCLUSIONS

We have simulated mono- and polydisperse quasi-two-dimensional random networks of soft-core conductive cylinders over a very wide range of aspect ratios (L/D = 25–800) and nanowire densities ($0.1 < N < 100N_c$). For

monodisperse networks, we observe a significant reduction in the percolation threshold with increasing aspect ratio. These percolation thresholds are in quantitative agreement with the widthless-stick result at $L/D > 100$ and are in excellent agreement with the finite-width excluded area model across all L/D's studied. We also report the conductivity exponent t as a function of the rod density in a contact-resistance dominated system ($R_c \gg R_{\text{rod}}$) for the highest rod densities studied to date. We find $t = 1.42$ at low densities ($N/N_c < 2$) and $t = 2$ at high densities ($N/N_c > 10$) with a crossover region at intermediate densities $2 < N/N_c < 10$. These results are consistent with recent numerical findings on the nonuniversality of the conductivity exponent in 2D widthless-stick systems [9,10,16]. In addition, we report t as a function of the aspect ratio, observing the same nonuniversality across the entire aspect-ratio range of $L/D = 25$–800. Finally, we generalize the finite-width excluded area model to account for arbitrary dispersity in rod lengths, finding a weight average dependence of the percolation threshold on the rod length. Moreover, we compare predictions from this generalized model to results from our simulations of rod networks with a bi-disperse distribution of rod lengths, obtaining good agreement between the two and further validating our model.

To summarize, the percolation threshold predictions from our simulations of quasi-2D rod networks and the generalized finite-width excluded area model presented in this paper provide experimentalists with valuable guidance to design and to optimize the properties of transparent conductors based on thin films of nanowires and nanotubes.

ACKNOWLEDGMENTS

This work was supported primarily by the MRSEC program of the National Science Foundation (Grant No. DMR-11-20901) and by the University Research Foundation of the University of Pennsylvania. The authors acknowledge M. C. Sherrott for her contributions during the initial stages of this work and Professor J. Li of the Department of Nuclear Science and Engineering at M.I.T. for the generous use of his group's computer cluster.

[1] D. S. Hecht, L. B. Hu, and G. Irvin, Adv. Mater. **23**, 1482 (2011).
[2] S. De and J. N. Coleman, MRS Bull. **36**, 774 (2011).
[3] A. Kumar and C. Zhou, ACS Nano **4**, 11 (2010).
[4] D. Stauffer and A. Aharony, *Introduction to Percolation Theory*, 2nd revised ed. (Taylor & Francis, London, 2003).
[5] G. E. Pike and C. H. Seager, Phys. Rev. B **10**, 1421 (1974).
[6] I. Balberg and N. Binenbaum, Phys. Rev. B **28**, 3799 (1983).
[7] I. Balberg and I. Balberg, N. Binenbaum, and C. H. Anderson, Phys. Rev. Lett. **51**, 1605 (1983).
[8] J. T. Li and S. L. Zhang, Phys. Rev. E **80**, 040104 (2009).
[9] J. Li and S.-L. Zhang, Phys. Rev. E **81**, 021120 (2010).
[10] M. Žeželj and I. Stanković, Phys. Rev. B **86**, 134202 (2012).
[11] M. Žeželj, I. Stanković, and A. Belić, Phys. Rev. E **85**, 021101 (2012).
[12] I. Balberg, C. H. Anderson, S. Alexander, and N. Wagner, Phys. Rev. B **30**, 3933 (1984).
[13] I. Balberg, Phys. Rev. B **31**, 4053 (1985).
[14] L. Hu, D. S. Hecht, and G. Gruner, Nano Lett. **4**, 2513 (2004).
[15] H. E. Unalan, G. Fanchini, A. Kanwal, A. Du Pasquier, and M. Chhowalla, Nano Lett. **6**, 677 (2006).
[16] P. Keblinski and F. Cleri, Phys. Rev. B **69**, 184201 (2004).
[17] R. M. Mutiso, M. C. Sherrott, J. Li, and K. I. Winey, Phys. Rev. B **86**, 214306 (2012).
[18] S. I. White, B. A. DiDonna, M. F. Mu, T. C. Lubensky, and K. I. Winey, Phys. Rev. B **79**, 024301 (2009).
[19] S. I. White, R. M. Mutiso, P. M. Vora, D. Jahnke, S. Hsu, J. M. Kikkawa, J. Li, J. E. Fischer, and K. I. Winey, Adv. Funct. Mater. **20**, 2709 (2010).
[20] R. M. Mutiso, M. C. Sherrott, A. R. Rathmell, B. J. Wiley, and K. I. Winey, ACS Nano (2013), doi: 10.1021/nn403324t.
[21] S. Kirkpatrick, Rev. Mod. Phys. **45**, 574 (1973).
[22] See Supplemental Material at http://link.aps.org/supplemental/10.1103/PhysRevE.88.032134 for representative renderings of simulated rod networks and additional discussion of the conductivity exponent.
[23] Y.-B. Yi, C.-W. Wang, and A. M. Sastry, J. Electrochem. Soc. **151**, A1292 (2004).
[24] M. S. Fuhrer, J. Nygard, L. Shih, M. Foreror, Y.-G. Yoon, M. S. C. Mazzoni, H. J. Choi, J. Ihm, S. G. Louie, A. Zettl, and P. L. McEuen, Science **288**, 494 (2000).
[25] A. Behnam, J. Guo, and A. Ural, J. Appl. Phys. **102**, 044313 (2007).
[26] S. Kumar, J. Y. Murthy, and M. A. Alam, Phys. Rev. Lett. **95**, 066802 (2005).
[27] I. Balberg, Phys. Rev. Lett. **59**, 1305 (1987).
[28] N. Johner, C. Grimaldi, I. Balberg, and P. Ryser, Phys. Rev. B **77**, 174204 (2008).
[29] G. Ambrosetti, N. Johner, C. Grimaldi, T. Maeder, P. Ryser, and A. Danani, J. Appl. Phys. **106**, 016103 (2009).
[30] E. C. Garnett, W. Cai, J. J. Cha, F. Mahmood, S. T. Connor, M. G. Christoforo, Y. Cui, M. D. McGehee, and M. L. Brongersma, Nat. Mater. **11**, 241 (2012).
[31] L. B. Hu, H. S. Kim, J. Y. Lee, P. Peumans, and Y. Cui, ACS Nano **4**, 2955 (2010).
[32] J. Y. Lee, S. T. Connor, Y. Cui, and P. Peumans, Nano Lett. **8**, 689 (2008).
[33] A. Bid, A. Bora, and A. K. Raychaudhuri, Phys. Rev. B **74**, 035426 (2006).
[34] M. R. Hestenes and E. Stiefel, J. Res. Natl. Bur. Stand. **49**, 409 (1952).
[35] S. M. Bergin, Y. H. Chen, A. R. Rathmell, P. Charbonneau, Z. Y. Li, and B. J. Wiley, Nanoscale **4**, 1996 (2012).
[36] J. Lee, P. Lee, H. Lee, D. Lee, S. S. Lee, and S. H. Ko, Nanoscale **4**, 6408 (2012).
[37] H. Wu, L. B. Hu, M. W. Rowell, D. S. Kong, J. J. Cha, J. R. McDonough, J. Zhu, Y. A. Yang, M. D. McGehee, and Y. Cui, Nano Lett. **10**, 4242 (2010).
[38] P. Lee, J. Lee, H. Lee, J. Yeo, S. Hong, K. H. Nam, D. Lee, S. S. Lee, and S. H. Ko, Adv. Mater. **24**, 3326 (2012).

[39] D. Zhang, R. Wang, M. Wen, D. Weng, X. Cui, J. Sun, H. Li, and Y. Lu, J. Am. Chem. Soc. **134**, 14283 (2012).
[40] A. Aharony and J. P. Hovi, Phys. Rev. Lett. **72**, 1941 (1994).
[41] J. P. Hovi and A. Aharony, Phys. Rev. E **53**, 235 (1996).
[42] R. M. Ziff and M. E. J. Newman, Phys. Rev. E **66**, 016129 (2002).
[43] L. Onsager, Ann. N.Y. Acad. Sci. **51**, 627 (1949).
[44] Z. Neda, R. Florian, and Y. Brechet, Phys. Rev. E **59**, 3717 (1999).
[45] L. Berhan and A. M. Sastry, Phys. Rev. E **75**, 041120 (2007).
[46] W. Xia and M. F. Thorpe, Phys. Rev. A **38**, 2650 (1988).
[47] A. V. Kyrylyuk and P. van der Schoot, Proc. Natl. Acad. Sci. USA **105**, 8221 (2008).
[48] R. H. J. Otten and P. van der Schoot, Phys. Rev. Lett. **103**, 225704 (2009).
[49] B. Nigro, C. Grimaldi, P. Ryser, A. P. Chatterjee, and P. van der Schoot, Phys. Rev. Lett. **110**, 015701 (2013).
[50] A. P. Chatterjee, J. Chem. Phys. **132**, 224905 (2010).